

Design and analysis of a truncated elliptical-shaped chipless RFID tag

Ameer Taimour KHAN¹, Yassin ABDULLAH², Sidra FARHAT^{3,*} , Wasim NAWAZ⁴ ,
Usman RAUF¹

¹School of Computational Sciences, The University of Faisalabad, Faisalabad, Pakistan

²Department of Telecommunication Engineering, University of Engineering and Technology, Taxila, Pakistan

³ACTSENA Research Group, Department of Telecommunication Engineering

University of Engineering and Technology, Taxila, Pakistan

⁴Özyeğin University, İstanbul, Turkey

Received: 19.08.2020

Accepted/Published Online: 11.12.2020

Final Version: 30.11.2021

Abstract: This article presents a novel polarization-insensitive chipless radio frequency identification tag having an encoding capacity of 11 bits. The proposed resonator design comprises discontinuous arc slots forming truncated elliptically shape offering 1:1 slot to bit correspondence with suppressed unwanted harmonic resonances. Electromagnetic performance analysis of the proposed tag design is done over an ungrounded Rogers RT duroid[®] 5880 laminate. The overall tag design covers a footprint of $15 \times 15 \times 0.508 \text{ mm}^3$ offering convincingly appreciable bit density of 4.88 bits/cm^2 . The realized tags are analyzed for real-world electromagnetic performance resulting in an agreement between measured and computed results. The proposed work finds its applications in the food and beverage industry.

Key words: Chipless tag, data encoding circuits, electromagnetics, radar cross section, radio frequency identification

1. Introduction

Over time, the diversity of communication sector has expanded affluently. A new concept of involving pervasive surroundings of an environment comprising of objects capable of transceiving the information through the wireless or wired connectivity has opened a new paradigm in the area of communication known as the Internet of things (IoT). Being one of the emerging technologies, IoT is augmented with ambient intelligence [1]. The main idea acting as the foundation for IoT is the creation and connectivity of smart objects, devices, vehicles, and handheld devices [2]. Research and development of these devices is the need of the hour to minimize the human-to-human or human-to-machine intervention. These devices are capable of receiving, transmitting, and processing the data offering an intelligent and smart solution. Radio frequency identification (RFID) is an emerging technology, which works on the contactless data capturing techniques [1]. RFID has found enormous whereabouts as an enabling technology for the deployment of an IoT framework, including smart monitoring, asset tracking, and object identification [3]. Moreover, RFID systems are deployed for improvement in healthcare services and consistent tracking of vital signs at individual level [4]. Offering lucrative features such as nonlinear sight communication [5], extensive read range [6], inexpensive realization, fast interrogation process, and reliable exchange of information, RFID is acting as a beacon in the present tech era, proving to be one of the massively adaptive technologies of the future [7]. On the other hand, limitations of the chipless RFID tag entail a lack of international standardization in frequency allocation, data loss due to signal collision to read multiple

*Correspondence: sidrafarhat63@yahoo.com

tags simultaneously, and electromagnetic disturbances arising due to the surrounding environment. Moreover, error in manufacturing is also a hindrance in the chipless RFID tag technology [8].

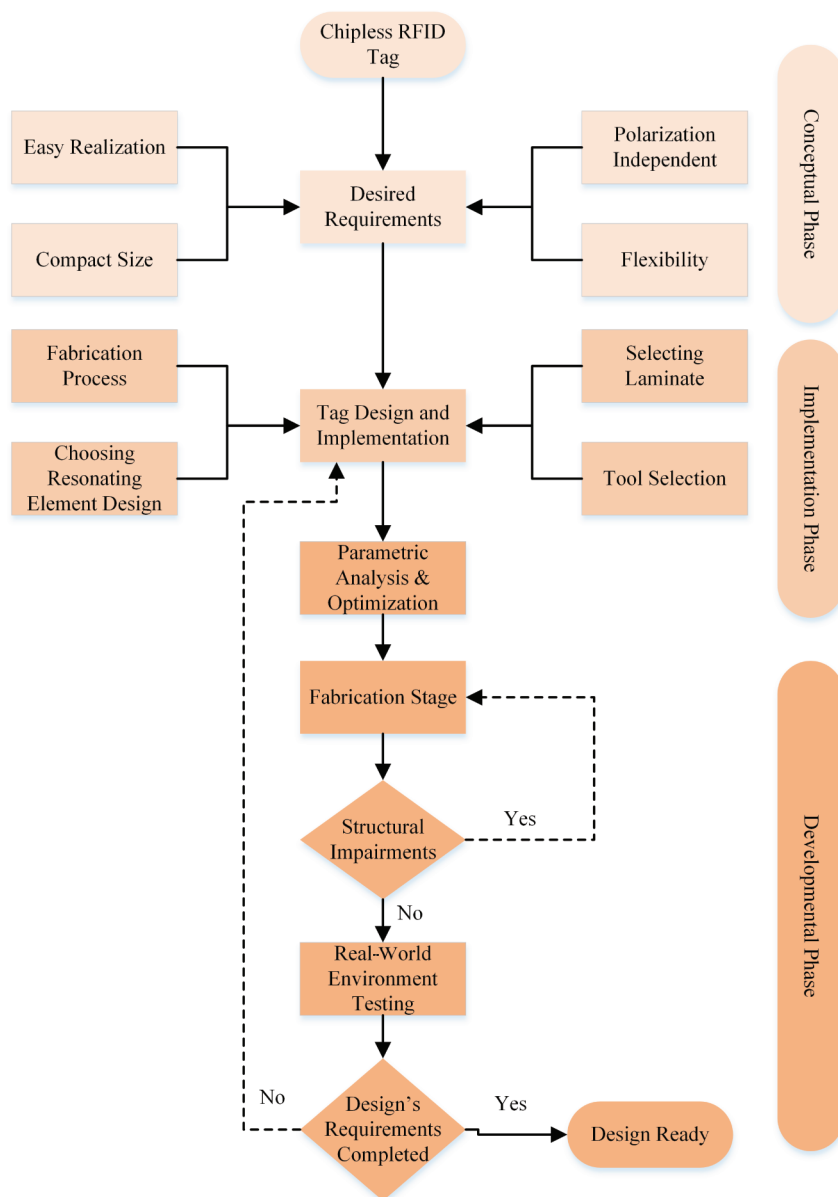


Figure 1. Design methodology.

An overall RFID system comprises a transponder commonly known as tag and an interrogator or reader connected to a host computer. The RFID tags are primarily classified into chip-based and chipless tags depending upon their working principle. A chipped RFID tag stores the information in an integrated circuit (IC), while in the chipless tag the data is stored in a passive encoder [9] using a particular type of radiating structures [10]. These structures vary in terms of shape and design, such as L and I [11], rectangular [12], triangular [13], and bow-tie-shaped [14].

This article proposes a compact frequency-domain-based chipless RFID tag with robust readable features. The electromagnetic performance of the design is examined using a variety of parameters including the absence or presence of high-order spectral harmonics, interresonating element coupling, polarization insensitivity, and bit density. The tag works on the principle of absorption and reflection of the interrogated electromagnetic waves that is eventually symbolized in the form of bit ‘1’ and bit ‘0’, respectively.

Recently reported work in chipless RFIDs is mainly focused on frequency-selective-surface-based tag realization using either rigid substrate [13–18] or deployment of expensive inks [19] such as silver nanoparticle ink [11, 20]. The authors in [19] and [21] suggest that silver nanoparticle-based layers are toxic and not recommended for tagging purposes for food and beverage industry. This work proposes low-cost chipless RFID tags using nonrigid laminate produced through cost-effective negative etching process. The tags consist of copper conductive layer instead of silver nanoparticles due to its nontoxic nature for beverage and food products. Moreover, owing to regular symmetry of the design the proposed tag remains invulnerable to a variety of incident angles of electromagnetic wave resulting in robust readability of tagged objects. Such applications require the tags to possess longer shelf-life with simple production processes, and cost effectiveness for mass production. The proposed designs are implemented on substrates with high tensile strength and are manufactured using negative etching process. Distinct absorption peaks for bit encoding, clearly identifiable in the RCS response, are obtained while maintaining polarization-insensitive features. Keeping in view the requirements, a flowchart encompassing the conception, design, fabrication, and performance analysis is illustrated in Figure 1.

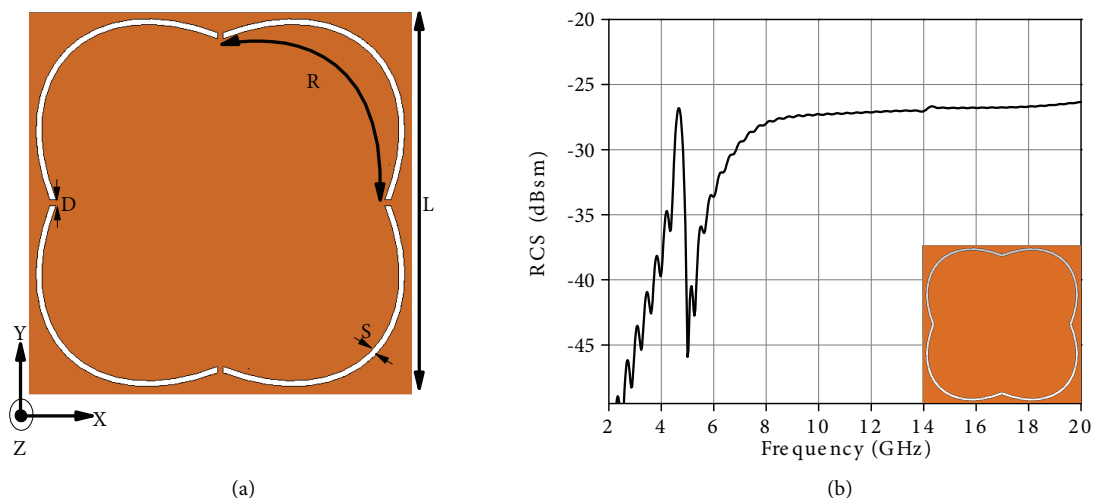


Figure 2. (a) Resonating element design, (b) RCS response without discontinuity.

2. Resonating element design

The proposed resonator is essentially truncated elliptical-shaped slots with a rotation of $+45^\circ$ and -45° along the XY-vertices of the structure as illustrated in Figure 2a. Geometric parameters involved in the construction of the slot design include the curve length R and slot width given by S . A discontinuity D is the length of truncation along the XY-vertices of the elliptical shape introduced to minimize the unwanted harmonic resonances.

A nontruncated elliptical slot exhibits unwanted RCS response as illustrated in Figure 2b, limiting the utilization of the operating frequency band and giving rise to spurious resonant peaks.

A discontinuity D that truncates the edges that reduces surface current elements related to the harmonic resonances is introduced. This results in a suppression of 2nd and 3rd harmonic resonances in the RCS response as illustrated in Figure 3a.

The surface current distribution of the outermost loop of the finalized resonator design at its fundamental frequency of 9.22 GHz is shown in Figure 3b. The results depict that the current distribution near the points labelled as D is maximum showing inductive effect, while in the vicinity of point D' the current distribution is minimum indicating the presence of capacitive nature. The simultaneous presence of inductive and capacitive effect across the resonating element is responsible for the resonance at the specific convinced value of frequency.

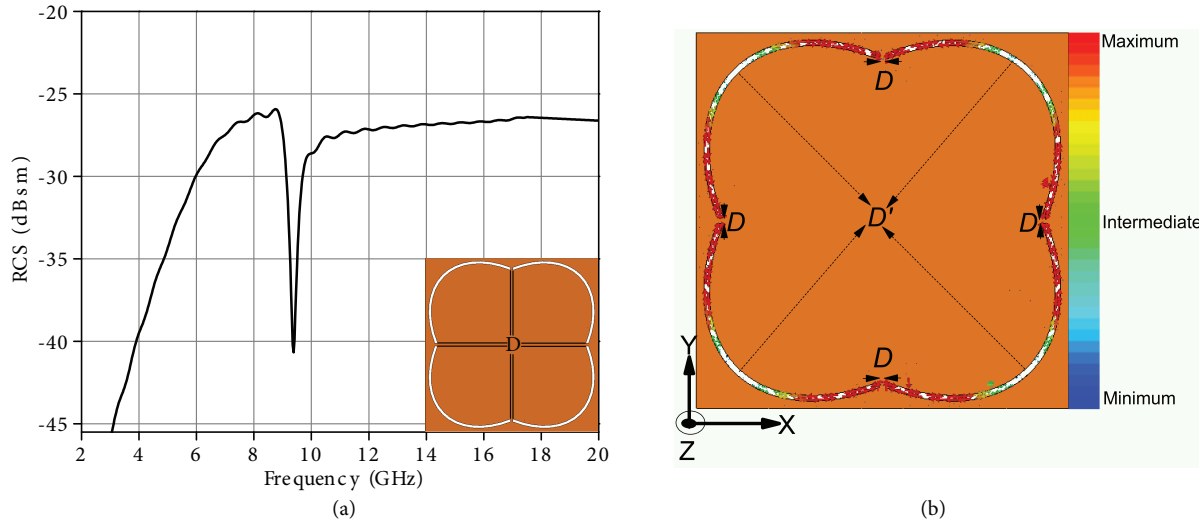


Figure 3. (a) RCS response of the proposed resonating element, (b) surface current distribution.

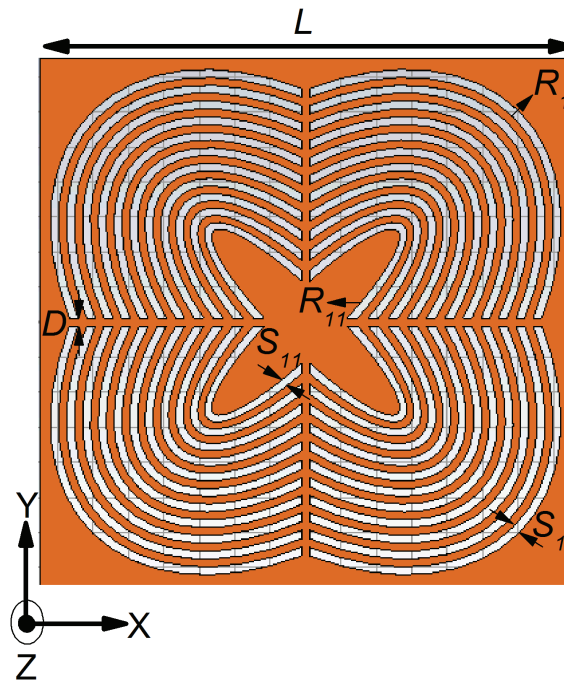


Figure 4. Proposed tag design.

3. Overall tag design

The proposed design covers a minuscule footprint of $15 \times 15 \text{ mm}^2$ and nested with eleven truncated elliptical slot-based structures as shown in Figure 4. Interresonating element space is function of length S . The gap is chosen such that the mutual coupling amongst closely placed slots limited to the extent that distinguishable resonances are observed and 1:1 slot to resonance in the RCS response is ensured. A total number of 2^{11} combinations are possible and 2048 unique IDs can be generated through the tag. Each slot of the resonating element is responsible for the corresponding resonance in the RCS response of the tag, hence symbolizing each bit. Presence or absence of each corresponding slot represents a bit '1' and bit '0', respectively. Unique tag IDs can be generated through a combination of removal and addition of corresponding slot elements.

Specific values for the geometric parameters of the overall design are provided in Table 1. Resonating element denoted by R_1 in Figure 4 corresponds to the most significant bit (MSB), whereas R_{11} is related to the least significant bit (LSB). Moreover, R_1 , being the largest element, resonates at the lowest frequency in the operating band and R_{11} at the highest. Tag samples of the proposed design realized on Rogers RT/duroid® 5880 are placed beside a 100 South Korean won coin for size comparison as shown in Figure 5. The tag design is fairly compact as illustrated in the figure.

Table 1. Optimized parameters of the tag (mm).

Parameters	Dimensions	Parameters	Dimensions
R_1	12.18	R_2	11.49
R_3	10.81	R_4	10.12
R_5	9.44	R_6	8.78
R_7	8.14	R_8	7.51
R_9	6.92	R_{10}	6.38
R_{11}	5.92	$S_1=S_2$	0.24
$S_5=S_6$	0.25	$S_7=S_8$	0.26
S_9	0.27	S_{10}	0.28
S_{11}	0.29	D	0.23
$S_3=S_4$	0.24	L	15



Figure 5. Fabricated samples of the proposed design.

4. Results and discussion

This section covers the electromagnetic analysis of the proposed tag design. The computer-aided simulations were orchestrated using the computer simulation tool Micro Wave Studio (CST® MWS®). Electromagnetic performance of the proposed design is analyzed using Rogers RT/duroid® 5880. Figure 6a. illustrates RCS response of the reported tag with all 1's, completely shorted, i.e. all zeros, tag IDs 11001100111 and 01101101111. Table 2 provides an insight into the proposed design's properties in terms of different parameters.

Table 2. Optimized parameters of the tag (mm).

Parameters	Proposed tag
Substrate	Rogers RT/duroid® 5880.
Thickness (mm)	0.508
Permittivity	2.2
Loss tangent	0.0009
Fabrication process	Copper etching
Conductor thickness (mm)	0.035
Frequency band (GHz)	9.22–18.44
Capacity (bits)	11
Flexible substrate	Yes

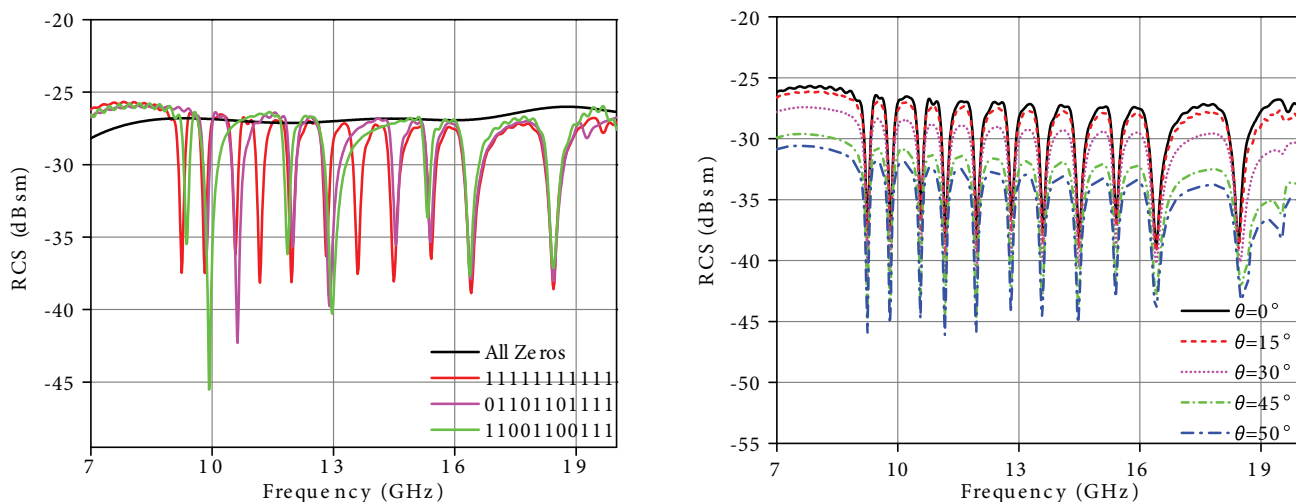


Figure 6. (a) RCS response for arbitrary bit sequences, (b) Oblique incidence performance of the tag.

The proposed design is also scrutinized for its electromagnetic performance at a variety of incident angles, when placed in a slanting position. It is evident from Figure 6b that articulated chipless RFID tag exhibits stable readability up to 50°. Moreover, a downward shift in the electromagnetic signature is perceived with respect to change in the incoming illuminated angles from 0° to 50° within the assigned operational frequency band.

The experimental setup employed for the real-world environment is the same as that deployed in [22]. The setup consists of a pair of linearly polarized transmitting and receiving horn antennas, different fabricated samples of tag along with a network analyzer Rohde and Schwarz® (R&S) ZVB-20. Figure 7 depicts the block diagram for the experimental setup.

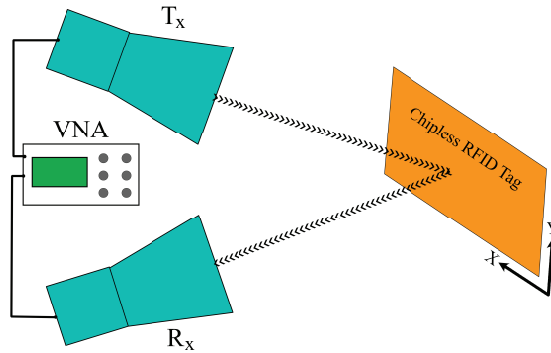


Figure 7. Block diagram of the experimental setup.

Experimental measurements are performed using continuous wave stepped frequency technique by sweeping the frequency over the operational frequency band. A 0 dBm transmit power is used to detect the backscattered signal from the chipless RFID tag using vector network analyzer (VNA) R&S® ZVB-20. The tag is kept at the far field distance calculated using the Fraunhofer distance formula given in Equation(1) [20].

$$R = \frac{2D^2}{\lambda}, \tag{1}$$

where D is the largest dimension of the tag and λ is the wavelength. λ can be calculated using

$$\lambda = \frac{C}{f}, \tag{2}$$

where C is speed of light and f is the central frequency of the operating band. S_{21} measurements are recorded: 1) in the absence of the RFID tag, $S_{21}^{isolation}$, 2) in presence of conducting metallic plate, S_{21}^{ref} with same dimensions as that of the tag. The RCS of the metallic plate σ^{ref} is calculated using Equation (3) [21].

$$\sigma^{ref} = 4\pi \left[\frac{Area\ of\ Plate}{\lambda} \right]^2 \tag{3}$$

Finally, the overall RCS of the tag can be calculated after measuring S_{21} of the chipless RFID tag (S_{21}^{tag}) and plugging in previously mentioned calculated parameters in Equation (4) [19].

$$\sigma^{tag} = \left[\frac{S_{21}^{tag} - S_{21}^{isolation}}{S_{21}^{ref} - S_{21}^{isolation}} \right]^2 \cdot \sigma^{ref} \tag{4}$$

The graphical comparison of the computed and measured results for the tag IDs 111111111111, 11001100111, and 01101101111 realized over Rogers RT/duroid® 5880 exhibits a good deal of agreement with one another, which can be seen in the Figures 8–8 (c), respectively.

A minor difference in resonant frequencies is noticed between the computed and experimentally measured results. It arises from the structural impairments introduced during the fabrication process of the tag. Moreover,

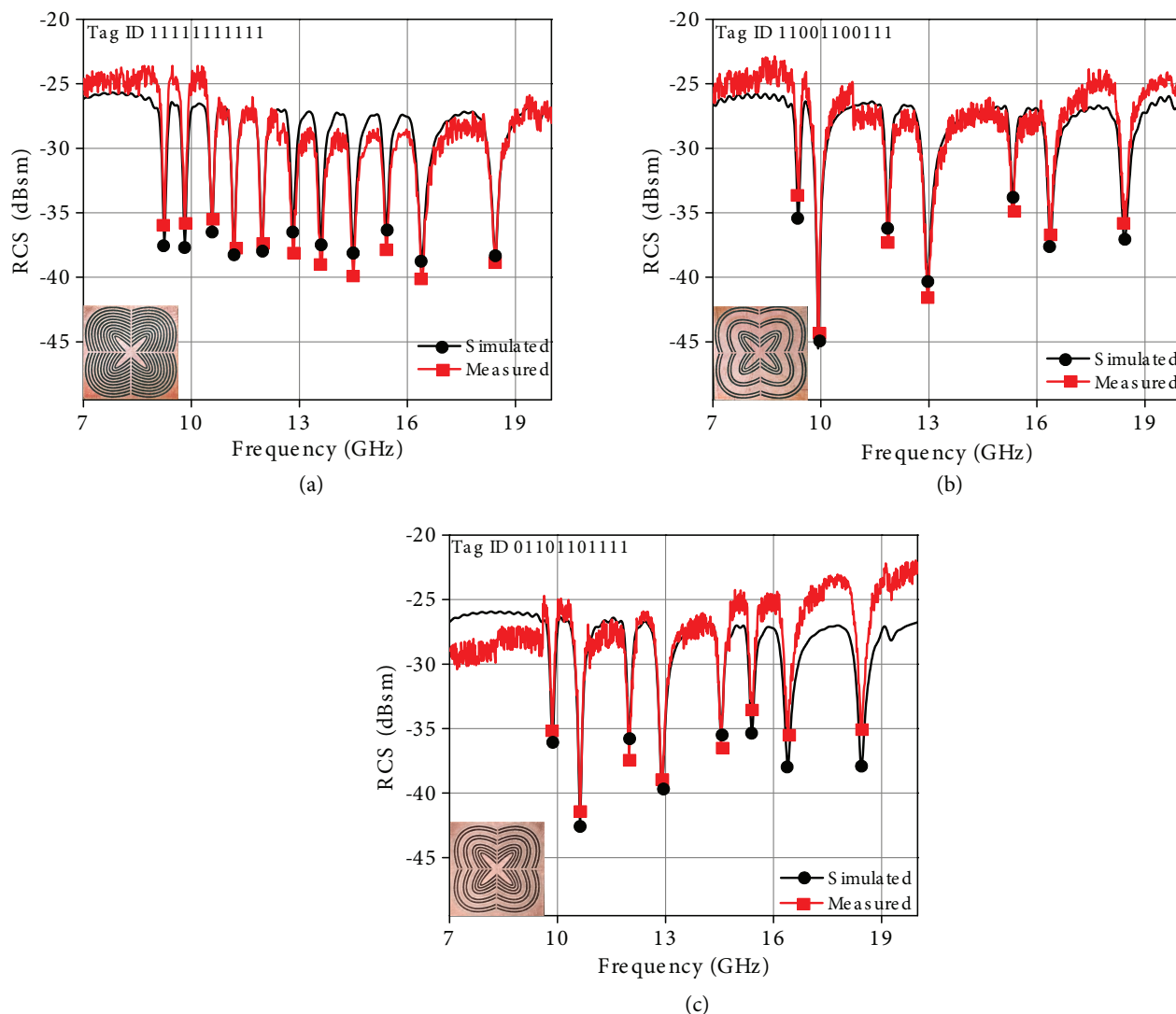


Figure 8. (a)RCS of the Tag ID111111111111, (b) RCS of the Tag ID110011001111, (c) RCS of the Tag ID011011011111.

variation in transmitting and receiving horn antennae gain over the operating frequency range and undesired environmental effects also contribute to a slight difference between the experimental and computed results. The proposed tag design realized on Rogers RT/duroid[®]5880 depicts good absorbance of EM waves resulting in higher RCS absorption levels and operates in the frequency band of 9.22–18.44 GHz. The encoded sequences are distinguishable in spectral domain as distinct dips in the RCS response validating the suitability of the design.

The reported tag is equiangular and equilateral in geometrical architecture, which imparts the polarization insensitivity to the design. The RCS response of a single resonant element with $R=12.18$ mm Rogers RT/duroid[®]5880 substrates is shown in Figure 9. It is evident from the figure that for distinct values of interrogating electromagnetic (EM) wave, the RCS response of the tag using V and H probes is consistent.

Table 3 presents a comparison of the proposed tag with existing work in the literature. In [11], a polarization-sensitive tag with a capacity of 08 bits offering a bit density of 1.12 bit/cm^2 having printed silver nanoparticles as a conducting layer is presented; this increases the cost of the tag and also is not recommended

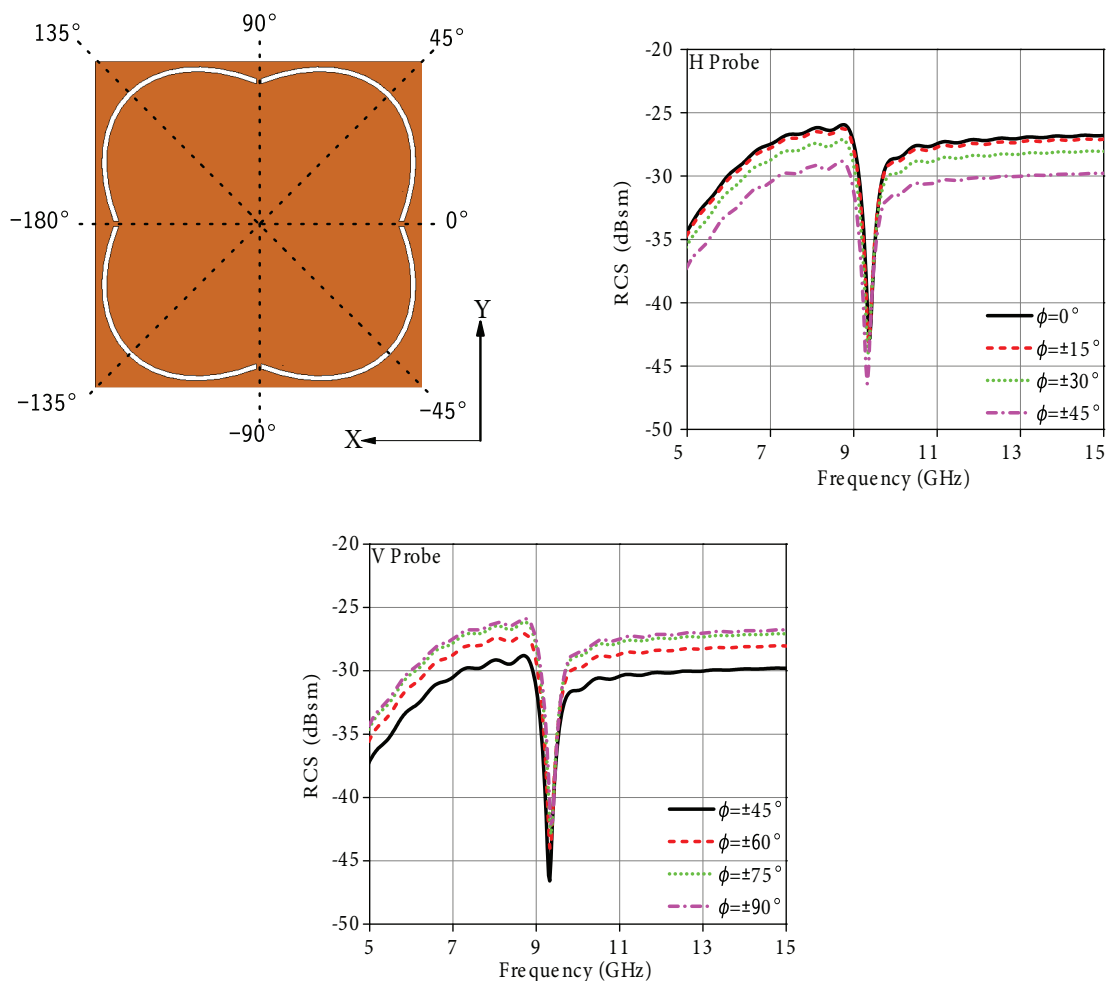


Figure 9. Design symmetry and polarization insensitivity.

for food and beverage articles. In [12], a copper etched polarization-insensitive tag with a coding capacity of 05 bits covering a vast footprint of 9 cm² is discussed. In [13], a triangular-shaped tag realized on the FR-4 substrate having a bit density of 1.21 bit/cm² is demonstrated. In [14], a copper etched chipless RFID tag with bow tie structure having an encoding capacity of 16 bits is achieved at the cost of a tremendous area covering 11.55 cm². A 5-bit polarization-dependent tag realized over a rigid substrate is reported in [15]. In [16], a T-shaped chipless RFID tag having a bit density of 4.44 bit/cm² with a polarization dependency is presented. A chipless RFID tag with 08 encoded bits posing a bit density of 0.45 bit/cm² realized using copper as a conducting layer is suggested in [17]. A rigid circular-shaped tag possessing an encoding capacity of 09 bits is reported in [18]. The authors in [20] present a nanosilver-particle-based printed tag with an area of 29.4 cm². A 10-bit elliptical-shaped chipless RFID tag covering an area of 3.64 cm² demonstrating a bit density of 2.74 bit/cm² is presented in [23]. Circular-shaped resonating element tags with bit densities of 2.11 bit/cm² and 3.80 bit/cm² are discussed in [25] and [27], respectively. The authors in [26] expound a tag over an area 42.64 cm² with an encoding capacity of 05 bits. Moreover, an expensive printed nanosilver ink particle is deployed as a conducting layer in the formulation of the tag. In [28], a polarization-sensitive tag with a bit density of

3.40 bit/cm² is designed. A cobwebbed-shaped polarization-insensitive chipless RFID tag having a bit density of 2.26 bit/cm² is reported in [29]. A quick response (QR) incorporated a chipless RFID tag with a huge area of 30.25 cm² involving a complex mechanism of labeling and reading of QR code is presented in [30]. A 06-bit square-looped tag having a bit density of 0.24 bit/cm² is represented in [31]. This study proposes a novel, robust, low-cost, and polarization-insensitive chipless RFID tag. The nonrigid, low-profile, and compact chipless RFID tag maintaining a footprint of 1.5 x 1.5 cm², capable of encoding 11 bits augment a bit density of 4.88 bit/cm².

Table 3. Comparison with other reported work.

Resonator shape	Encoded bits	Size (cm ²)	Bit density (bit/cm ²)	Polarization insensitivity	Flexible laminate	Conducting layer
L and I [11]	08	7.14	1.12	No	Yes	Printed silver nanoparticle
Rectangular [12]	05	9.00	0.55	Yes	No	Copper etched
Triangular [13]	10	8.25	1.21	No	No	Copper etched
Bow tie [14]	16	11.55	1.03	No	No	Copper etched
C-shaped [15]	05	8.00	1.25	No	No	Copper etched
T-shaped [16]	10	2.25	4.44	No	No	Copper etched
E-shaped [17]	08	17.7	0.45	No	No	Copper etched
Circular [18]	09	14.04	1.56	Yes	No	Copper etched
Dual rhombic [20]	16	29.4	0.54	No	Yes	Printed silver nanoparticle
Elliptical [23]	10	3.64	2.74	Yes	Yes	Copper etched
Circular [25]	19	9.00	2.11	Yes	Yes	Copper etched
Octagonal [26]	05	42.64	0.11	Yes	Yes	Printed silver nanoparticle
Circular loop [27]	09	2.36	3.80	Yes	Yes	Conductive ink
Inverted C-shaped [28]	12	3.52	3.40	No	Yes	Copper etched
Cobwebbed [29]	12	5.29	2.26	Yes	Yes	Copper etched
QR with square loop [30]	08	30.25	3.9	No	Yes	Copper etched
Square [31]	06	24.75	0.24	No	Yes	Copper etched
Proposed	11	2.25	4.88	Yes	Yes	Copper etched

5. Conclusions

A novel, flexible, fully passive, and polarization-insensitive chipless RFID tag is presented in this article. Incorporating the on-off keying technique, the proposed tag offers an encoding capacity of 2¹¹ distinct combinations for labeling and identification of various articles. The etching process employed to realize the proposed design, covering a minuscule footprint of 1.5 × 1.5 cm² is cost-effective for mass production. Moreover, the tag offers an appreciable bit density of 4.88 bit/cm². The peculiar geometrical structure of the resonating element of the proposed design augments polarization insensitivity to the tag. The formulated tag is realized on flexible ungrounded Rogers RT Duroid® 5880 laminate, which renders its deployment over irregular and conformable surfaces. The tag consists of a copper conductive layer instead of silver nanoparticles due to its nontoxic nature for beverage and food products, which makes it a suitable candidate in the food and beverage industry. Owing to lucrative features like robustness, high tensile strength resulting in a longer shelf-life, low cost, low profile, single layer, orientation, and polarization independence, it finds potential wear about in different IoT applications like inventory management of retail stores, smart cities, and pharmaceutical warehouses.

Author contributions

A.T.K is responsible for the tag design, fabrication, manuscript preparation. Y.A. is responsible for the tag design and manuscript preparation. S.F. analyzed the acquired data and the results and revised the manuscript. W.N. is responsible for the tag fabrication and measurements and helped in revising the article critically. U.R. supervised the whole research and provided intellectual suggestions.

References

- [1] Al-Fuqaha A, Guizani M, Mohammadi M, Aledhari M, Ayyash M. Internet of things: a survey on enabling technologies, protocols, and applications. *IEEE Communications Surveys & Tutorials* 2015; 17: 2347-2376.
- [2] Singh D, Tripathi G, Jara AJ. A survey of Internet-of-things: future vision, architecture, challenges and services. *IEEE World Forum on Internet of Things (WF-IoT) Seoul* 2014; 287-292.
- [3] Solic P, Blazevic Z, Skiljo M, Patrono L, Colella R et al. Gen2RFID as IoT enabler: characterization and performance improvement. *IEEE Wireless Communication* 2017; 24: 33-39.
- [4] Castillejo J, Martinez J, Molina R, Cuerva A, Integration of wearable devices in a wireless sensor network for an e-health application. *IEEE Wireless Communication* 2013; 20: 38-49.
- [5] Öktem R, Aydın E. An RFID based indoor tracking method for navigating visually impaired people. *Turkish Journal of Electrical Engineering and Computer Sciences* 2010; 18: 185-196.
- [6] Sevinç Y, Kaya A. Reconfigurable antenna structure for RFID system applications using varactor-loading technique. *Turkish Journal of Electrical Engineering and Computer Sciences* 2012; 20: 453-462.
- [7] Yu F, Qian Z, Wang X, Liu G. Identifying the unknown tags in a large RFID system. *China Communication* 2017; 14: 135-145.
- [8] Kaur M, Sandhu M, Mohan N, Sandhu PS. RFID technology principles, advantages, limitations & its applications. *International Journal of Computer and Electrical Engineering* 2011; 3: 151-157.
- [9] Herrojo C, Mata-Contreras J, Núñez A, Paredes F, Ramon E et al. Near-field chipless-RFID system with high data capacity for security and authentication applications. *IEEE Trans on Microwave Theory and Technology* 2017; 65: 5298–5308.
- [10] Aslam B, Khan UH, Habib A, Amin Y, Tenhunen H. Frequency signature chipless RFID tag with enhanced data capacity. *IEIC Electron Express* 2015; 12: 20150623-20150623.
- [11] Habib A, Asif R, Fawwad M, Amin Y, Ioo J et al. Directly printable compact chipless RFID tag for humidity sensing. *IEIC Electron Express* 2017; 14: 20170169-20170169.
- [12] Costa F, Genovesi S, Monorchio A. A chipless RFID based on multiresonant high-impedance surfaces. *IEEE Trans Microwave Theory Technology* 2013; 61: 146-153.
- [13] Rauf S, Riaz MA, Shahid H, Iqbal MS, Amin Y et al. Triangular loop resonator based compact chipless RFID tag. *IEIC Electron Express* 2017; 14: 20161262-20161262.
- [14] Xu L, Huang K. Design of compact trapezoidal bow-tie chipless RFID tag. *International Journal of Antennas and Propagation* 2015.
- [15] Mumtaz M, Amber SF, Ejaz A, Habib A, Jafri SI et al. Design and analysis of C shaped chipless RFID tag. *Wireless Systems and Networks (ISWSN) IEEE* 2017; 26: 1-5.
- [16] Riaz MA, Shahid H, Aslam SZ, Amin Y, Akram A et al. Novel T-shaped resonator based chipless RFID tag. *IEIC Electron Express* 2017; 14: 20170728- 20170728.
- [17] Sumi M, Dinesh R, Nijas CM, Mridula S, Mohanan P. High bit encoding chipless RFID tag using multiple E shaped microstrip resonators. *Progress in Electromagnetics Research* 2014; 61: 185-196.

- [18] Babaeian F, Karmakar NC. Hybrid Chipless RFID Tags-A Pathway to EPC Global Standard. *IEEE Access* 2018; 6: 67415-67426.
- [19] Magdassi S, Grouchko M, Kamyshny A. Copper nanoparticles for printed electronics: routes towards achieving oxidation stability. *Materials* 2010; 3: 4626-4638.
- [20] Habib A, Sohaira A, Akram A, Azam MA, Amin Y et al. Directly printable organic ASK based chipless RFID tag for IoT applications. *Radioengineering* 2017; 26: 453.
- [21] George S, Lin S, Ji Z, Thomas JR, Li LJ et al. Surface defects on plate-shaped silver nanoparticles contribute to its hazard potential in a fish gill cell line and zebrafish embryos. *ACS Nano* 2012; 6: 3745-3759.
- [22] Vena A, Perret E, Tedjini S. Chipless RFID tag using hybrid coding technique. *IEEE Trans Microwave Theory Technology* 2011; 59: 3356-3364.
- [23] Jabeen I, Ejaz A, Akram A, Amin Y, Loo J et al. Elliptical slot based polarization insensitive compact and flexible chipless RFID tag. *International Journal of RF and Microwave Computer-Aided Engineering* 2019; e21734.
- [24] Balanis CA. *Antenna Theory: Analysis and Design*, 4th ed. Wiley, 2016.
- [25] Vena A, Perret E, Tedjini S. High-capacity chipless RFID tag insensitive to the polarization. *IEEE Trans on Antennas and Propagation* 2012; 60: 4509-4515.
- [26] Betancourt D, Haase K, Hübner A, Ellinger F. Bending and folding effect study of flexible fully printed and late-stage codified octagonal chipless RFID tags. *IEEE Trans on Antennas and Propagation* 2016; 64: 2815-2823.
- [27] Martinez M, van der Weide D. Compact slot-based chipless RFID tag. *RFID Technology and Applications Conference (RFID-TA), IEEE* 2014; 26: 233-236.
- [28] Ali A, Jafri SI, Habib A, Amin Y, Tenhunen H. RFID humidity sensor tag for low-cost applications. *Applied Computational Electromagnetics Society Journal* 2017; 32: 3745-3759.
- [29] Khan AT, Riaz MA, Shahid H, Amin Y, Tenhunen H et al. Design and analysis of cobwebbed shaped chipless RFID tag. *Microwave Journal* (accepted 2019, to be published).
- [30] Shahid H, Riaz MA, Akram A, Amin Y Loo J et al. Novel QR-incorporated chipless RFID tag. *IEIC Electron Express* 2019; 16: 20180843-20180843.
- [31] Shahid L, Shahid H, Riaz MA, Naqvi SI, Jamil M et al. Chipless RFID tag for touch event sensing and localization. *IEEE Access* 2019.